

Structural uncertainty in projecting global fisheries catches under climate change



William W.L. Cheung^{a,*}, Miranda C. Jones^{a,b}, Gabriel Reygondeau^a, Charles A. Stock^c, Vicky W.Y. Lam^{a,d}, Thomas L. Frölicher^e

^a Nippon Foundation-Nereus Program, Institute for the Oceans and Fisheries, The University of British Columbia, Vancouver, BC, Canada V6 T 1Z4

^b Zoology Department, University of Cambridge, Downing Street, Cambridge CB2 3EJ, UK

^c Geophysical Fluid Dynamics Laboratory, National Oceanographic and Atmospheric Administration, Princeton, NJ, USA

^d Sea Around Us, Institute for the Oceans and Fisheries, The University of British Columbia, Vancouver, BC, Canada

^e Environmental Physics, Institute of Biogeochemistry and Pollutant Dynamics, ETH Zürich, Zürich, Switzerland

ARTICLE INFO

Article history:

Received 7 August 2015

Received in revised form

19 December 2015

Accepted 31 December 2015

Keywords:

Dynamic Bioclimate Envelope Model

Climate change

Uncertainty

Habitat suitability

MAXENT

AquaMaps

ABSTRACT

The global ocean is projected to be warmer, less oxygenated and more acidic in the 21st century relative to the present day, resulting in changes in the biogeography and productivity of marine organisms and ecosystems. Previous studies using a Dynamic Bioclimate Envelope Model (DBEM) projected increases in potential catch in high latitude regions and decreases in tropical regions over the next few decades. A major structural uncertainty of the projected redistribution of species and fisheries catches can be attributed to the habitat suitability algorithms used. Here, we compare the DBEM projections of potential catches of 500 species of exploited marine fishes and invertebrates from 1971 to 2060 using three versions of DBEM that differ by the algorithm used to predict relative habitat suitability: DBEM-Basic, DBEM-Maxent and DBEM-Aquamaps. All the DBEM models have similar skill in predicting the occurrence of exploited species and distribution of observed fisheries production. Globally, the models project a decrease in catch potential of 3% to 13% by 2050 under a high emissions scenario (Representative Concentration Pathway 8.5). For the majority of the modelled species, projections by DBEM-Maxent are less sensitive to changes in ocean properties than those by DBEM-Aquamaps. The mean magnitude of projected changes relative to differences between projections differ between regions, being highest (>1 times the standard deviation) in the tropical regions and Arctic Ocean and lowest in three of the main Eastern Boundary Upwelling regions, the eastern Indian Ocean and the Southern Ocean. These results suggest that the qualitative patterns of changes in catch potential reported in previous studies are not affected by the structural uncertainty of DBEM, particularly in areas where catch potential was projected to be most sensitive to climate change. However, when making projections of fish stocks and their potential catches using DBEM in the future, multiple versions of DBEM should be used to quantify the uncertainty associated with structural uncertainty of the models. Overall, this study contributes to improving projection of future changes in living marine resources by exploring one aspect of the cascade of uncertainty associated with such projections.

© 2016 Published by Elsevier B.V.

1. Introduction

Biogeochemical properties of the oceans have been altered by CO₂ emissions from human activities since the beginning of the 20th century (Gattuso et al., 2015; IPCC, 2013). Particularly, the ocean is becoming warmer, less oxygenated, and (Portner et al., 2014), resulting in changes in the distribution (Cheung et al.,

2013a; Pinsky et al., 2013; Poloczanska et al., 2013), community structure (Beaugrand et al., 2015), trophodynamics (Ainsworth et al., 2011; Kirby and Beaugrand, 2009; Stock et al., 2014a), and productivity of marine organisms and ecosystems (Gattuso et al., 2015; Portner et al., 2014). Consequently, fisheries will be impacted through changes in distribution and potential catches of exploited marine species (Barange et al., 2014; Cheung et al., 2011, 2010). Previous studies using a Dynamic Bioclimate Envelope Model (DBEM) project increases in catch in high latitude regions and decreases in tropical systems by the mid-21st century (Cheung et al., 2010, 2011).

* Corresponding author. Tel.: +1 6048273756.

E-mail address: w.cheung@oceans.ubc.ca (W.W.L. Cheung).

The DBEM is a numerical approach to project the effect of climate change on exploited species and consists of two main components: (1) predicting species' habitat suitability in each spatial grid; (2) simulating spatial population dynamics of fish stocks that include population growth, movement and dispersal of adult and larvae, as well as the ecophysiological effects of temperature, oxygen and acidity on body size, growth, mortality and reproduction (Cheung et al., 2013b). In addition, DBEM takes into account changes in net primary production (NPP) across space and time that affect an ecosystem's capacity to support fish stocks and alter fisheries catch potential (Fernandes et al., 2013). Thus, the projected redistribution of fisheries catch potential is in part due to poleward shifts in the distributions of exploited fish stocks that result in invasion of warmer-water species into higher latitude regions and local extinction in tropical waters (Jones and Cheung, 2015), and in part to changes in primary productivity (Cheung et al., 2011).

The prediction of species' habitat suitability under changing ocean biogeochemical properties can potentially alter projections of catch potential by DBEM and may be an important source of uncertainty (Jones et al., 2015). Habitat suitability in DBEM is predicted based on species' preferences to environmental conditions, inferred by overlaying current distributions with gridded environmental data (Cheung et al., 2008c). Alternative methods of predicting habitat suitability are available and the application of these methods may generate substantially different projections of biogeography (Elith and Leathwick, 2009). At a regional scale, a case study of projecting future catch potential under climate change scenarios in the UK waters using DBEM and two alternative species distribution models suggests that the projected trends are consistent between models, while the magnitude and finer scale patterns of change may vary substantially (Jones et al., 2015). However, the effects of using different habitat suitability algorithms in projecting global change in fisheries catch under the DBEM framework have not been explored previously.

In this study, we examined the effects of using alternative numerical procedure to predict species' habitat suitability on projected changes in catch of exploited marine fishes and invertebrates under the DBEM framework. Specifically, we compared the DBEM projections using the original habitat suitability algorithm as described in Cheung et al. (2011) with projections that were driven by predicted habitat suitability from Maxent and Aquamaps (Jones and Cheung, 2015). We evaluated the degree of agreement between the predicted potential catch with the total maximum fisheries catches of the modeled species as reported in the *Sea Around Us* dataset (www.searounds.org). We hypothesized that the projected direction of changes in global and regional total potential catch is consistent between alternative algorithms while the projected magnitude of change is more sensitive to alternative habitat suitability predictions. If such hypotheses are supported by this study, it would imply that the general pattern of projected potential catch under climate change showed in previous studies using DBEM projections, e.g., Lam et al. (2014), are robust to alternative structures of DBEM while there is a need to further explore other sources of variability and uncertainties associated with the projections (Cheung et al., 2016).

2. Methods

2.1. Dynamic Bioclimate Envelope Model (DBEM)—Basic structure

We used the DBEM to simulate changes in distribution, abundance and catches of exploited marine fishes and invertebrates. The structure of the DBEM is described in Cheung et al. (2011) and we summarize pertinent aspects of the model here.

2.1.1. Current species distribution

The current distributions of commercially exploited species, representing the average pattern of relative abundance in recent decades (i.e., 1970–2000), were produced using an algorithm developed by the *Sea Around Us* Project (see Close et al., 2006; Cheung et al., 2008b; www.searounds.org). The algorithm estimates the relative abundance of a species on a 0.5° latitude \times 0.5° longitude grid based on the species' depth range, latitudinal range, known Food and Agriculture Organization statistical areas and polygons encompassing their known occurrence regions. The distributions were further refined by assigning habitat preferences to each species, such as affinity to shelf (inner, outer), estuaries, and coral reef habitats. The required habitat information was obtained from FishBase (www.fishbase.org) and SeaLifeBase (www.sealifebase.org), which contains key information on the distribution of the species in question, and on their known occurrence region.

2.1.2. Projecting future habitat suitability

We calculated an index of habitat suitability for each species (P) in each spatial cell i from temperature (bottom and surface temperature for demersal and pelagic species, respectively), bathymetry, specific habitats, salinity and sea ice with 30-year averages from 1971 to 2000 of outputs from Earth System Models (see Supplementary materials). The multiple of these five components resulted in the overall habitat suitability:

$$P_i = P(T_i, TPP) \cdot P(Bathy_i, MinD, MaxD) \cdot P(Habitat_{i,j}, HAssoc) \cdot P(Salinity_i, SAssoc) \cdot P(Ice_i, IceP) \quad (1)$$

where T is seawater temperature, $Bathy$ is bathymetry, $Habitat$ is the proportion of area of the habitat type j relative to the total seawater area of the cell i , Ice is sea ice extent, and $Salinity$ is the salinity class of cell i according to the Thalassic series (hyperhaline, metahaline, mixoeuhaline, polyhaline, mesohaline and oligohaline). For each species, TPP is temperature preference profile, $MinD$ and $MaxD$ are minimum and maximum depth limits, $HAssoc$ is habitat association index, and $SAssoc$ has a value of 1 or 0 indicating whether the species is or is not associated to the specific salinity classes, respectively, and $IceP$ is association to sea ice for polar species.

Specifically, DBEM estimated the temperature preference profile (TPP) of each species by overlaying the estimated species distribution (Cheung et al., 2008b; Close et al., 2006; Jones et al., 2012) with annual seawater temperature and calculated the area-corrected distribution of relative abundance across temperature for each year from 1971 to 2000, subsequently averaging annual temperature preference profiles (TPP). The TPP was calculated from the predicted average relative abundance (R_i) from the estimated current species distribution in temperature class i over the entire range:

$$TPP_i = \frac{R_i}{\sum R_i} \quad (2a)$$

$$R_i = \frac{Q_i}{A_i} \quad (2b)$$

where Q_i and A are the sum of relative abundance and range area from spatial cells within temperature class i .

A species' distribution was also limited indirectly by depth. Thus, there were lower and upper limits of water depth ($minD$ and $maxD$, respectively) outside of which a species does not occur i.e.:

$$P(Bathy, minD, maxD) = 1 \quad (3a)$$

if $Bathy \geq minD$ and $Bathy \leq maxD$

$$= 0 \quad \text{if } Bathy < minD \text{ or } Bathy > maxD \quad (3b)$$

However, marine species can survive in deeper waters than they currently occur to some extent. To reflect this, the model allows the species to move to area where depth is twice the maximum depth limit.

Each species was assigned an index of association (*HAssoc*) to one or more of the four habitat types: coral reefs, estuaries, seamounts and habitats that are none of the above. The index, scaled between 0 and 1, represents the relative density of a species in the particular habitat. It was assigned based on qualitative descriptions of the ecology of the species from FishBase or other publications and literature (see Close et al., 2006 for description of how this index is estimated). Distribution of relative abundance was then adjusted based on the habitat-association index and the global distribution of each habitat:

$$P(\text{Habitat}, \text{HAssoc}) = \text{Habitat} \cdot \text{HAssoc} \quad (4)$$

Polar ecosystems, and the distributions of their associated species, are largely shaped by the dynamics of sea ice (Longhurst 1981). In both the Arctic and Antarctic, primary productivity around sea ice is generally high. For instance, in the Antarctic, phytoplankton growth is enhanced by micronutrient delivery and stabilization of the water column associated with the influx of lower salinity but nutrient rich water from melting ice. This in turn forms the base of the foodweb which support fishes and mammals in polar ecosystems (Eicken 1992; Legendre et al. 1992; Longhurst 1981). Thus, polar fishes are generally distributed close to sea ice (Legendre et al. 1992; Fuiman et al. 2002). It is therefore reasonable to assume that environmental preferences of polar species are partly dependent on distance from sea ice. To be consistent with the current species distributions, which represent annual average, annual average sea ice extent was used. We calculated polar species' relative habitat suitability in relation to sea ice using similar algorithms as when calculating TPP. However, instead of seawater temperature, sea ice extent was used in Eq. (2).

2.1.3. Modelling changes in spatial population dynamics

Movement and dispersal of adults and larvae were modelled through advection-diffusion-reaction equation for larval and adult stages using the following equations, respectively.

$$\frac{\partial A}{\partial t} = \frac{\partial}{\partial x} \left(D \frac{\partial A}{\partial x} \right) + \frac{\partial}{\partial y} \left(D \frac{\partial A}{\partial y} \right) - \frac{\partial}{\partial x} (u \cdot A) - \frac{\partial}{\partial y} (v \cdot A) - \lambda \cdot A \quad (5a)$$

$$\frac{\partial A}{\partial t} = \frac{\partial}{\partial x} \left(D \frac{\partial A}{\partial x} \right) + \frac{\partial}{\partial y} \left(D \frac{\partial A}{\partial y} \right) \quad (5b)$$

where A was abundance. Horizontal diffusion was characterized by a diffusion parameter D . Diffusion coefficient, expressed in $\text{m}^2 \text{s}^{-1}$, is assumed to be a function of length scale of the spatial grid: $D = (1.1 \times 10^{-4}) \cdot GR \cdot 1.33$ where GR is the minimum grid resolution (Nahas et al., 2003). Pelagic larvae were assumed to be passively advected and diffused via ocean currents and associated mixing (Cheung et al., 2009, 2008b). The instantaneous rate of larval mortality and settlement is represented by $\lambda = 1 - e^{-(M_L + S_L)}$ where M_L and S_L are the natural mortality and settlement rates of larvae, respectively. Adult's natural mortality is implicit in the intrinsic rate of population increase (r , Eq. (8)). Advection was characterized by two surface current velocity parameters (u, v) that described the east-west and north-south current movement across a distance between centers of neighboring cells in the east-west and north-south directions (x, y respectively). The duration of the pelagic larvae phase was predicted from an empirical equation as a function of sea surface temperature (O'Connor et al., 2007). The default larval mortality and larvae settlement rate are 0.85 day⁻¹

and 0.2 day⁻¹, respectively (Cheung et al., 2008b). Sensitivity analysis suggests that the long-term (decadal) projection of DBEM is not sensitive to these two parameters (Cheung et al., 2008b).

For juvenile-adult stages, diffusion rate was dependent on habitat suitability (P) and a density-dependent factor (ρ) that was a function of the carrying capacity (θ), population density (ϕ) and mean weight (\bar{W}) in the spatial cell i :

$$D_i = \frac{D_0 \cdot m}{1 + e^{(\tau \cdot P_i \cdot \rho_i)}} \quad (6)$$

$$\rho_i = 1 - \frac{\phi_i}{(\theta_i / \bar{W}_i)} \quad (7)$$

The coefficients m and τ determined the curvature of the functional relationship between D , P , and ρ (Cheung et al., 2008b), and D_0 is the initial diffusion coefficient. Thus, diffusion rate in the cell increased as environmental conditions (habitat suitability and carrying capacity) became less favorable to the species. Also, as population density approached carrying capacity, the density dependent factor decreased in value and diffusion rate increased. A gradient of diffusion rate between neighboring cells resulted in net movement from less to more suitable habitats or from more crowded to less densely populated areas.

The carrying capacity of a spatial cell (θ_i) is assumed to be distributed in proportion to the product of habitat suitability (P_i) and net primary production (NPP_i). The total carrying capacity is an estimate of the global unfished biomass based on the average of the top-10 annual catches by weight of the modelled species in the world from 1950 to 2004 and their intrinsic population growth rate (Cheung et al., 2008a). We assumed that the average of the top-10 annual catches was roughly equal to the maximum sustainable yield (MSY) of the species. This may be an over-estimation of MSY if the high catches subsequently led to over-exploitation, or that it may under-estimate MSY if the species was under-exploited. However, this would not substantially alter the main results from DBEM, which focused largely on the relative changes across time instead of the absolute biomasses or catches. Assuming logistic population growth, unfished biomass (B_{unfished}) of a population was estimated from (see Haddon, 2010 equation 11.26):

$$B_{\text{unfished}} = \frac{4 \cdot \text{MSY}}{r} \quad (8)$$

The model simulated changes in relative abundance of a species by solving the advective-diffusive equation in Eq. (5) first, and then feeding the outputs into a logistic growth function:

$$\frac{dA_i}{dt} = \sum_{j=1}^N r \cdot A_j \cdot \left(1 - \frac{A_i}{(\theta_i / \bar{W})} \right) - F \cdot A_i \quad (9)$$

where A_i is the abundance in a $30' \times 30'$ cell i , r is the intrinsic population growth, determined through the Euler-Lotka method (see Cheung and Sumaila, 2015). F is the fishing mortality rate, and carrying capacity in biomass is converted to numerical abundance by dividing it with the estimated mean weight (\bar{W}).

In addition to the abundance (A), DBEM calculates a characteristic weight (W) representing the average mass of the population in cell i . The model simulated how changes in temperature and oxygen content (represented by O₂ concentration) would affect growth of the individuals using a sub-model derived from a generalized von Bertalanffy growth function (VBGF) (Cheung et al., 2013b):

$$W_t = W_\infty \cdot [1 - e^{-K \cdot (t - t_0)}]^{1/(1-a)} \quad (10)$$

where W_∞ is the asymptotic weight, and K is the von Bertalanffy growth parameter. For simplification, we assume that the scaling coefficient $a = 0.7$, although empirical studies show that a generally

Table 1

Parameters of the DBEM model.

Parameters	Symbols	Default values	Unit
Abundance	A	Derived	No. of individuals
Asymptotic weight	W_{inf}	Varies between spp.	kg
Average relative abundance in temperature class i	R_i	Derived	No. of individuals
Bathymetry	Bathy	Varies between cells	m
Biomass	B	Derived	t
Carry capacity	θ	Derived	t
Catch	C	Varies between spp.	t per year
Coefficients determine the curvature functional relationship between D , H , and ρ	m, k	2, 2	–
Coefficients of the generalized VBGF	g, h	Derived	$\text{kg year}^{-1}, \text{year}^{-1}$
Metabolic coefficients	j_1, j_2	4.5, 8	Kelvin
Density-dependent factor	ρ	Derived	–
Diffusion coefficient	D	Derived	$\text{m}^2 \text{s}^{-1}$
Current velocity	u, v	Varies between cells	m s^{-1}
East-west distance	x, y	Varies between cells	m
Fishing mortality rate	F	Derived	year^{-1}
Habitat association index	HAssoc	Varies between spp.	–
Habitat suitability index	P	Derived	–
Intrinsic population growth	r	Varies between spp.	year^{-1}
Depth limits	MaxD, MinD	Varies between spp.	m
Maximum sustainable yield	MSY	Varies between spp.	t year^{-1}
Mean body weight	\bar{W}	Derived	kg
Natural mortality rate	λ	Derived	year^{-1}
Number of grid cells	N	259,200	Count
Population density	ϕ	Varies between spp.	No. of individuals
Probability of growth transition	X	Derived	–
Proportion of area of the habitat to the total seawater area	Habitat	Varies between cells	–
Range area from spatial cells within temperature	A	Derived	m^2
Relative biomass	B	Derived	t
Sea ice extent	Ice	Varies between cells	Percentage cover
Seawater temperature	T	Varies between cells	Kelvin
Unfished biomass	B_{unfished}	Varies between spp.	t
Weight	W	Derived	kg
von Bertalanffy growth parameter	K	Varies between spp.	year^{-1}

varies from 0.50 to 0.95 between fish species (Pauly, 2010, 1981), with 2/3 corresponding to the special or standard VBGF.

The model predicts changes in VBGF parameters for each species according to changes in temperature, oxygen and pH in the ocean relative to the initial conditions, as:

$$W_{\infty} = \left(\frac{g \cdot [O_2] \cdot e^{-j_1/T}}{h \cdot [H^+] \cdot e^{-j_2/T}} \right)^{1/(1-a)} \quad (11)$$

$$K = k \cdot (1 - a) \quad (12)$$

in which metabolism is temperature dependent and aerobic scope is dependent on oxygen availability in water and maintenance metabolism is affected by physiological stress (e.g., increased acidity). Also, $j = Ea/R$ with Ea and R are the activation energy and Boltzmann constant, respectively, while T is temperature in Kelvin (see Table 1 for default values of j_1 and j_2). In addition, the aerobic scope of marine fishes and invertebrates decreases as temperature approaches their upper and lower temperature limits (Pörtner 2010). The coefficients g and h were derived from the average W_{∞} , K and environmental temperature (T_0) of the species reported in literature:

$$g = \frac{W_{\infty}^{1-a} \cdot K}{[O_2] \cdot e^{-j_1/T_0}} \quad (13a)$$

$$h = \frac{K/(1-a)}{[H^+] \cdot e^{-j_2/T_0}} \quad (13b)$$

Adult natural mortality rate (M) was estimated from an empirical equation (Pauly, 1980):

$$M = -0.4851 - 0.0824 \cdot \log(W_{\text{inf}}) + 0.6757 \cdot \log(K) + 0.4687 \cdot \log(T_i) \quad (14)$$

where T is the average water temperature in cell i .

The estimated growth parameters and natural mortality rate were used in calculating the average body weight of individuals in the population using the length-based life table as detailed in Cheung et al. (2011), where:

$$\bar{W} = \frac{\sum_y \sum_l W_l \cdot X_{l',l} \cdot e^{-M}}{\sum_y \sum_l X_{l',l} \cdot e^{-M}} \quad (15)$$

$X_{l',l}$ is the probability of an individual growing from length class l to l' in a time-step (y) as estimated from growth data (Chen et al., 2003; Sadovy et al., 2007) and W_l is the mean weight of length class l .

Thus, average body weight was dependent on temperature and oxygen level. Biomass (B) and catch (C) were then calculated from the population mean body weight (\bar{W}) and abundance:

$$B = A \cdot \bar{W} \quad (16a)$$

$$C = A \cdot F \cdot \bar{W} \quad (16b)$$

The model had a spin-up period of 100 years using the climatological average oceanographic conditions from 1971 to 2000, thereby allowing the population to reach equilibrium before it was perturbed with oceanographic changes. This basic version of DBEM is hereafter called DBEM-basic

2.2. DBEM—Alternative structure

We examined the effects of alternative prediction of species' habitat suitability on DBEM projections. Specifically, we used two other species distribution models (SDM), Maxent and AquaMaps, that had been tested and applied to a large number of exploited marine fishes and invertebrates in the world to infer their spatial distributions (Jones et al., 2012; Jones and Cheung, 2015; Kaschner et al., 2011; Rengstorf et al., 2013).

Maxent and AquaMaps use generative statistical procedures to determine species' environmental envelopes from species occurrence data and a suite of environmental variables. Species occurrence data are represented by presence data only, which is considered more appropriate when absence data are likely to be inaccurate. Although absence data are occasionally available for marine species, they are not available for many of the species modelled here. The two models, contrasting each other in the algorithms used (Jones et al., 2012), were applied to predict the "current" distributions of the set of species using 30-year averaged environmental data centered on 1985 (1971–2000) of the same variables that are used in DBEM-basic.

In the two alternative versions of DBEM (DBEM-Maxent and DBEM-AquaMaps), we assumed that the carrying capacity (θ) in each geographical cell of the ocean, as specified in Eqs. (6) and (7), was proportional to the habitat suitability index provided by Maxent and AquaMaps, respectively. Moreover, in both alternative DBEM versions, we did not consider the effects of changes in ocean properties on growth and body size. Other than these modifications, the other model structure and parameterization remained the same as the basic version of DBEM (Table 1).

2.2.1. DBEM-Maxent

The model Maxent (Phillips and Dudík, 2008) generated predictions of species' relative habitat suitability by associating species' occurrence data with the set of 1971–2000 averaged environmental variables (representing the 'current' time period) used in DBEM-basic. Maxent (Phillips et al., 2006) uses a complex generative approach (Phillips et al., 2006) to estimate the environmental co-variates conditioning species' presence from presence only occurrence data and a suite of environmental variables. The final prediction is based on the principle of maximum entropy, which specifies that the best approximation of an unknown distribution is the probability distribution with maximum entropy, or that closest to uniform (Phillips et al., 2006).

Models were constructed using Maxent version 3.3.3e with default parameters for a random seed, regularization parameter (1, included to reduce over-fitting), maximum iterations (500), convergence threshold (0.00001) and maximum number of background points (10,000 points which have not been recorded as present). The relative contribution of environmental variables to each iteration of the model was also carried out automatically. The model trained on the set of environmental variables representing the current time period was then 'projected' by its application to a set of the same environmental variables representing future ocean conditions from 1971 to 2060. The Maxent logistic output results in values lying between 0 and 1, and represents the relative suitability of each grid cell for each species, higher values indicating more suitable conditions and thus a higher likelihood of species occurrence. Detailed descriptions of the Maxent process are given in Elith et al. (2011), Phillips and Dudík (2008), and Phillips et al. (2006).

2.2.2. DBEM-AquaMaps

AquaMaps (Kaschner et al., 2011; Ready et al., 2010) uses a simple statistical approach to predict a species' distribution from occurrence data and the set of averaged environmental variables. AquaMaps is a presence only method, calculating a species environmental envelope using databases of species' occurrence points (Jones et al., 2012; Kaschner et al., 2011). An environmental envelop is constructed using a trapezoidal response curve, determined by a species' absolute and 'preferred' preference ranges. Relative environmental suitability is assumed to be uniformly high between preferred preference limits, while those outside absolute limits are assigned a probability of 0. Suitability decreases between absolute and preferred tolerance limits. Predictions of relative habitat suitability are generated for each environmental variable

and combined multiplicatively for an overall prediction of relative habitat suitability. Habitat suitability predictions are normalized to scale between 0 and 1.

2.3. Sample of species and their current distributions

We applied the three versions of DBEM to model a sample of species that contributed most to regional catches or the variation in species composition. First, we selected the species samples that would have the largest influences on the distribution and catches in each ocean basin, quantified via the Escoufier's equivalent vectors (Escoufier, 1970) for the occurring species in each ocean region [delineated by the Food and Agriculture Organization (FAO) Statistical Areas]. The Escoufier's equivalent vector was calculated based on the most significant variables (sensu Shannon, 2001) from a multivariate data frame according to a principal component analysis. In this study, the variables being examined were the predicted relative habitat suitability of each species occurring in each FAO area. High values of Escoufier's equivalent vectors suggest a more representative set of variables (predicted habitat suitability) in a multivariate matrix. Subsequently, for each FAO area, the pool of species representing more than 95% of the total cumulated Escoufier's equivalent vectors was selected. These operations were iterated for each FAO area and model. Second, we identified the top ten species with the largest fisheries catches between 2000 and 2006 in each FAO area according to the Sea Around Us catch database (www.searounds.org). If these fisheries important species were not already sampled from the analysis using the Escoufier's equivalent vector, we included them for further analysis. In total, these procedures resulted in a sample of 500 species.

Basic biological and biogeographical parameters for the sample of species, including growth parameters and length-weight relationships, were obtained from FishBase (www.fishbase.org) and SeaLifeBase (www.sealifebase.org), which contained key information on the distribution of the species in question. For DBEM-Maxent and DBEM-Aquamaps, species occurrence data were obtained from the Ocean Biogeographic System (OBIS, <http://www.iobis.org>, accessed in 2013). Erroneous data points were removed using known environmental preferences and geographic limits, obtained from FishBase (Froese and Pauly, 2011) and Sealifebase (www.sealifebase.org), before being spatially aggregated on a 0.5° latitude × 0.5° longitude grid.

2.4. Scenarios

We projected changes in potential fisheries catches from 1971 to 2060 under a scenario of future changes in GHG emissions under a business-as-usual scenario. Changes in surface and bottom sea water temperature, oxygen concentration, salinity, net primary production, surface advection, and sea ice concentration under the Representative Concentration Pathways (RCP) 8.5 were based on outputs from the Geophysical Fluid Dynamics Laboratory Earth System Model (GFDL ESM2M; Dunne et al., 2012). We note that the resolution of ESM2M is, like other ESMs used for climate change projections (Stock et al., 2011), coarse. Resolution at high latitudes is ~1°, with latitudinal resolution gradually increasing to 1/3° near the equator. Limitations imposed by this resolution will be discussed. The outputs were re-gridded onto a 0.5° × 0.5° grid map of the world ocean using the nearest neighbour method and values in some coastal cells were extrapolated using bilinear extrapolation.

We applied a constant fishing mortality rate across the geographic range of each species. Specifically, to predict the theoretical maximum potential catches, we assumed that fishing was approximately at maximum sustainable yield (MSY) throughout the simulation. Given that logistic population growth was assumed in all versions of DBEM, fishing mortality rate at MSY for each species

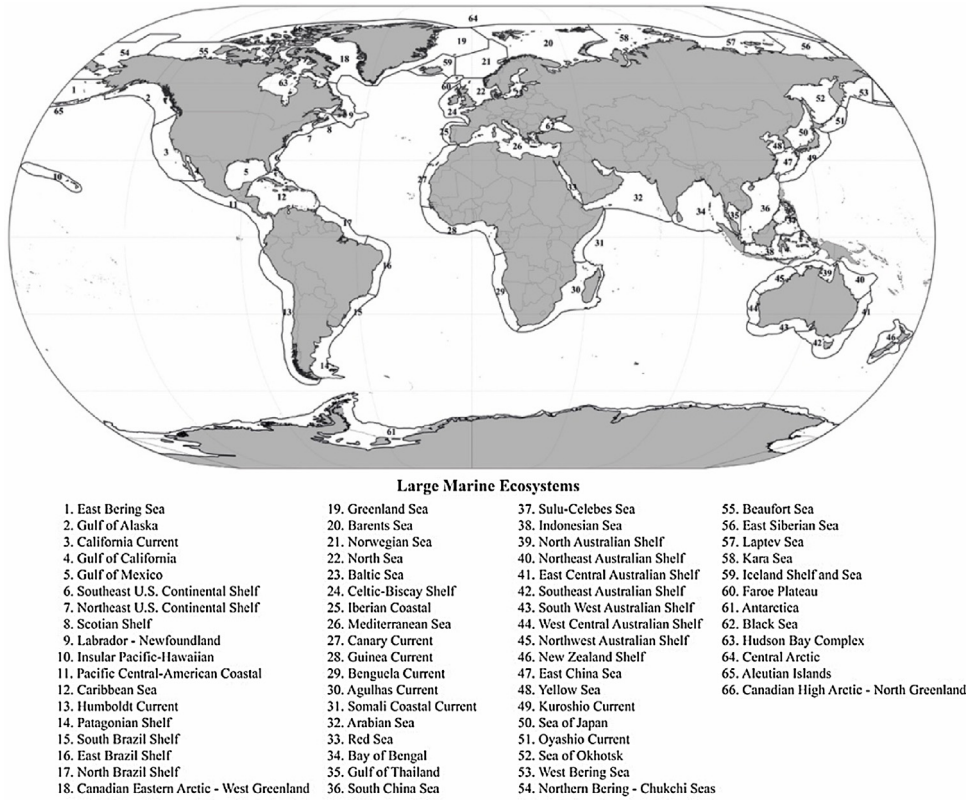


Fig. 1. Boundary of the 66 Large Marine Ecosystems (<http://lme.edc.uri.edu/>).

was equal to half of the intrinsic population growth rate of the species. i.e., $F=r/2$.

2.5. Benchmarking

We compared the predicted catch from the three DBEM models against reported maximum catches in each Large Marine Ecosystem (LME, Fig. 1) from the *Sea Around Us* global catch database. We calculated the average annual predicted catches from each model for all the modeled species from 1971 to 2000. For each LME, we also calculated the total reported catch from the sample of species and computed the average annual catch from the ten highest catches in each LME. As LMEs differ substantially in size, we normalized the catches by LME area. We calculated the Pearson correlation coefficient between the predicted and reported catches to test the ability of the model to capture relative catch values between LME, deemed most essential for projecting relative changes in catch. To further examine the accuracy of the model, we tested whether the slopes of the linear regression between the predicted and reported catches were significantly different from 1. We also compared the accuracy between the models by calculating the mean absolute error (MAE) between the predicted and observed catches. i.e., the mean of the absolute values of the difference between predicted and observed catches (log-transformed).

In addition, we compared the performance of each model in predicting the distribution of individual species. For each of the modelled species, we compared the predicted distribution (average between 1971 and 2000) with observed occurrence records using the Area Under Curve (AUC) of the Receiver Operating Characteristics (ROC) test. Observed ROC curves were generated for each species, expressed as the plotted difference between true positive rate (number of true occurrences/total number of predicted occurrences) and the false positive rate (number of false predicted occurrences/total number of absence). An AUC of the ROC curve of

0.5 indicated that predictions were no better than random; higher AUC values indicated increasing prediction performance. Finally, to assess the potential for results to be skewed by unreliable distributions, we calculated the percentage of maximum catch potential from species with AUC value that is lower than 0.5.

Using each version of DBEM, we projected and compared future changes in total potential catch and their variability in each large marine ecosystem over a 20 year period centered around 2050 (2041–2060) relative to 1971–2000 under RCP 8.5 scenario. We evaluated the correlation of projected potential catches between the models in each LME. We also calculated the projected mean annual catch (summing across species) and the standard deviation across the three versions of DBEM. We then examined the spatial pattern of “signal-to-noise” ratio across LMEs, expressed as the ratio of mean annual projected potential catch to their standard deviation across the three versions of DBEM.

3. Results

The predicted current maximum catch potentials from the three DBEM versions were all significantly correlated with reported maximum catch across LMEs ($p < 0.05$, Pearson test between the predicted and reported mean annual catch potential, Fig. 2, Table 2). Specifically, predicted catch potential from DBEM-Basic correlated most strongly with reported catches ($r = 0.79$) and DBEM-Maxent ($r = 0.78$), followed by DBEM-Aquamaps ($r = 0.65$).

Predicted catches for LMEs in the Arctic and Antarctic regions generally had the largest disagreement with reported catches across all three models. Specifically, the residuals of the linear regressions were highest in the Antarctic (LME number 61), Central Arctic Ocean (64) and the Beaufort Sea (55) Large Marine Ecosystems (see Supplementary information). Also, as the slope of the regression lines were significantly lower than 1 (one-tail test of slope < 1 , $p < 0.0001$), the models systematically underestimated

Table 2

Test statistics of Pearson correlation test between maximum catch potential estimated based on DBEM projections and reported catches.

Model	Mean	Correlation coefficient			p-Value
		Lower confident limit	Upper confident limit		
DBEM-Basic	0.79	0.67	0.87		<0.0001
DBEM-AquaMaps	0.65	0.48	0.77		<0.0001
DBEM-Maxent	0.78	0.66	0.86		<0.0001

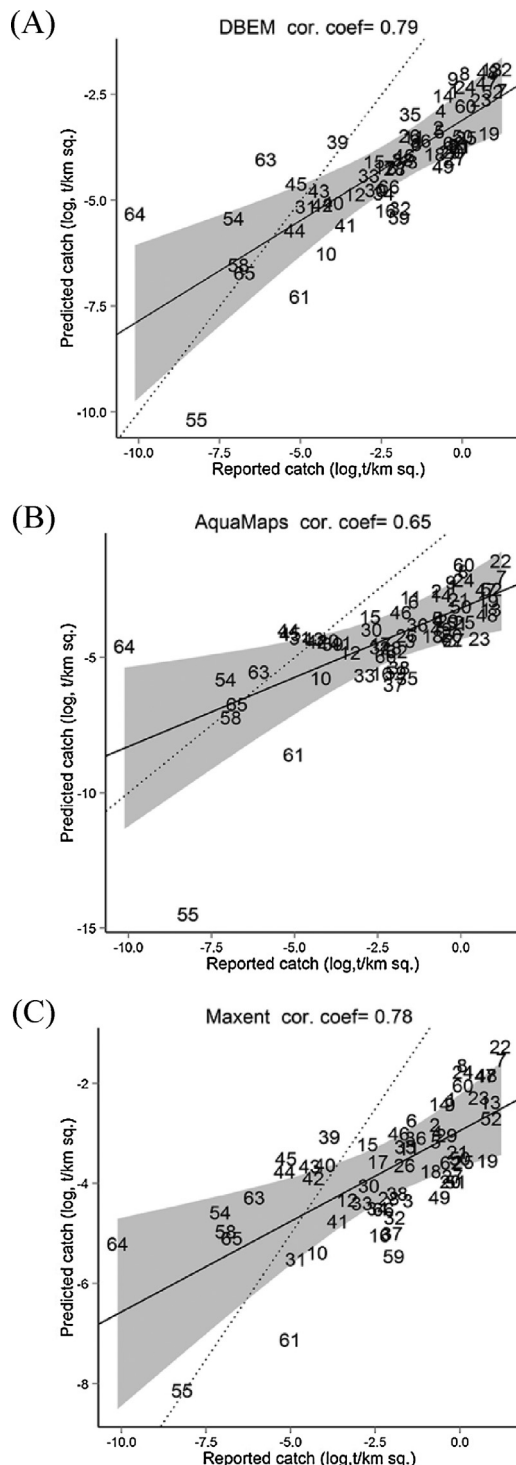


Fig. 2. Relationship between reported maximum catch and projected potential catches by Large Marine Ecosystems from the three versions of DBEM: (A) DBEM-Basic, (B) DBEM-AquaMaps and (C) DBEM-Maxent. The grey area represents the 95% confident interval of the estimation from the linear regression. The dotted lines represent 1:1 between predicted and reported catches.

the potential catches of LME with high maximum production. The mean absolute error is lowest for DBEM-Maxent (2.2), followed by DBEM-Basic (2.3) and DBEM-AquaMaps (2.5).

Predicted distributions of the majority (>90%) of the modelled species for all the DBEM models had AUC values higher than 0.5 (Fig. 3) indicating better predicting performance than random. Species with prediction distributions that performed poorly ($AUC \leq 0.5$) contributed only a small fraction to the total global maximum catch potential: 0.04%, 0.2% and 0.2% for DBEM-Basic, DBEM-AquaMaps and DBEM-Maxent, respectively. Overall, DBEM-Basic performed better than DBEM-AquaMaps and DBEM-Maxent in terms of AUC statistics.

The three models projected decreases in global potential catch by 2050 while the projections varied in the magnitude of the decrease (Fig. 4). DBEM-Basic, DBEM-Aquamaps and DBEM-Maxent projected decreases in catch potential by 6%, 13% and 3% respectively under RCP 8.5 scenario by 2050 (2041–2060 average) relative to 1970–2000 period. Projected changes in potential catch by the three models in each LME are presented in the Supplementary materials. In contrast, in a 100 year simulation without changes in ocean conditions, the relative abundance and catch of each species remained unchanged when simulations continued under constant ocean conditions.

Regionally, projected changes in potential catch correlated closely between DBEM-Basic, DBEM-Aquamaps and DBEM-Maxent in the majority of LMEs, although DBEM-Aquamaps differed more from DBEM-Basic and DBEM-Maxent (Fig. 5, also see Supplementary materials). A total of 56, 44 and 52 LMEs had correlation coefficients above 0.5 for the comparison between DBEM-Basic vs DBEM-Maxent, DBEM-Basic vs DBEM-Aquamaps and DBEM-Maxent vs DBEM-Aquamaps, respectively. Moreover, all three models agreed in the direction of projected change in catch

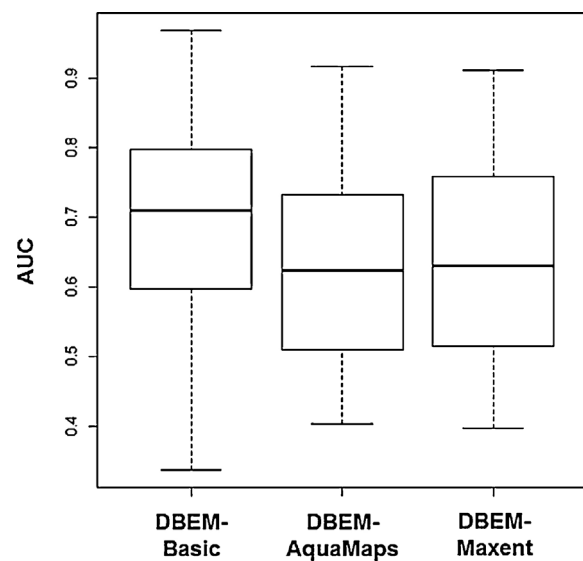


Fig. 3. Area under curve (AUC) of the Receiver Operating Curve of the predicted distributions from DBEM-Basic, DBEM-AquaMaps and DBEM-Maxent compared with occurrence records. The plot is based on the AUC values from all the studied species.

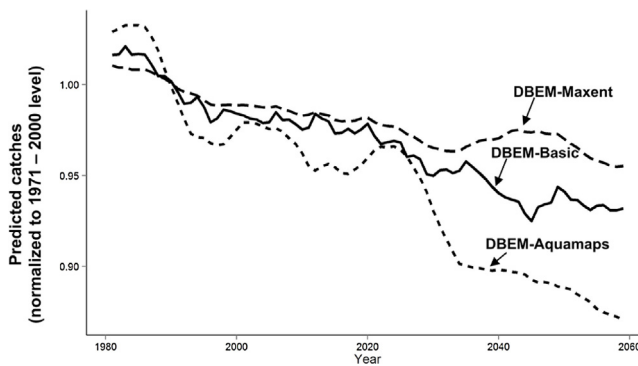


Fig. 4. Projected potential catch relative to the 1971–2000 period under RCP 8.5 future greenhouse gas scenario by DBEM-Basic (solid line), DBEM-Aquamaps (dotted line) and DBEM-Maxent (dash line). The projected catch time-series were filtered using a 10-year running mean.

potential in 54 out of 66 LMEs while the remaining had at least one model that showed different projected directions. The LMEs in which the three DBEM models differed most widely in terms of direction of changes are Humboldt Current (13), East-Central Australia (41), Southeast Australia (42) and Antarctic (61).

The signal-to-noise ratio, indicated by mean relative changes in potential catch (average across the three DBEM versions) over their standard deviation, by 2041–2060 relative to 1971–2000 under the RCP 8.5 scenario, was generally highest in many LMEs in the tropics and the Arctic Ocean (Fig. 6). Particularly, potential catch was projected to decrease most (more than 30%) in the Gulf of Pacific Central America Coastal, Guinea Current and Sulu-Celebes Sea LMEs where the signal-to-noise ratio is moderately high (mean changes were 1 to 3 times the standard deviations). In addition, the Arctic Ocean LMEs, including the Norwegian Sea, Chukchi Sea, West Bering Sea and the West Greenland Shelf LMEs also had high signal-to-noise ratio. In contrast, some of the eastern boundary

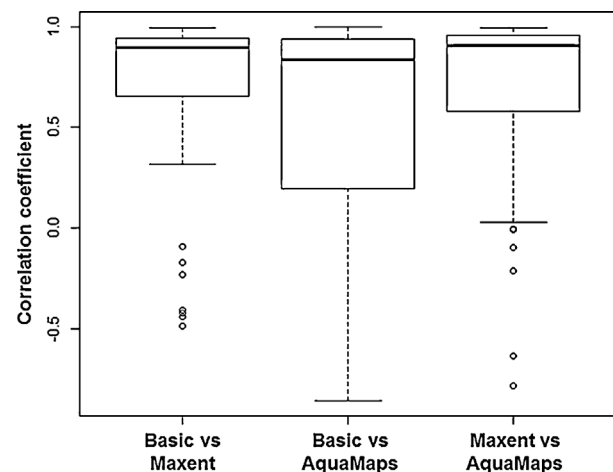


Fig. 5. Correlation coefficients of the projected relative changes in potential catch from 1971 to 2060 under RCP 8.5 by LMEs comparing outputs from DBEM-Basic vs DBEM-Maxent, DBEM-Basic vs DBEM-AquaMaps and DBEM-Maxent vs DBEM-AquaMaps. Open circles are data point which lie beyond the extremes of the whiskers.

upwelling systems such as the California Current, Humboldt Current, Canary Current LMEs, and the Antarctic Ocean LMEs had high differences in the projections between the three models.

4. Discussion

The use of several DBEM algorithms confirmed a robust trend toward a global decrease in potential catch of marine exploited species. The magnitude of projected global declines, however, varied between algorithms. This was particularly true at regional scales, where variation in trends between algorithms were often large relative to the projected mean changes.

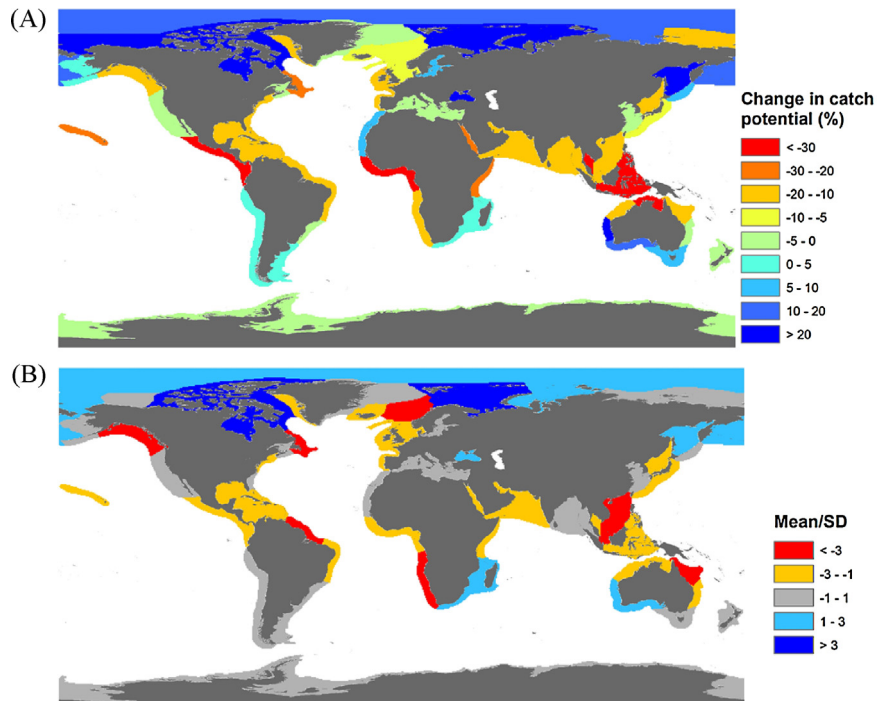


Fig. 6. Multi-model ensemble projections of changes in potential catch by 2050 (2041–2060) relative to present day (1971–2000) under the RCP 8.5 scenario: (A) mean percentage changes in potential catch and (B) ratio of mean changes to standard deviation (SD) between models as a proxy of signal-to-noise ratio. Values that are below -1 or above $+1$ suggest that the decrease and increase in potential catches (signal), respectively, is higher than the variation between the three models (noise).

Projections by DBEM-Maxent had relatively modest declines, whereas projections by DBEM-Aquamaps were more sensitive to changes in ocean properties. Aquamaps predicts habitat suitability using trapezoidal environmental preferences envelopes. This results in sharp decreases in habitat suitability in the marginal habitats of a species. In contrast, Maxent used a non-parametric algorithm based on the maximum entropy theory that allows the model to fit complex non-linear relationships with multiple environmental variables and their co-variation (Phillips et al., 2006). Habitat suitability predicted by Maxent is generally a continuous function with large areas of relatively low habitat suitability and results in high goodness-of-fit to observed occurrence of the modelled species, making the DBEM projections with Maxent more conservative. This may explain the relatively lower sensitivity of the projected change in catch potential over time from DBEM-Maxent than DBEM-Basic and DBEM-Aquamaps. In addition, DBEM-basic incorporates temperature-dependent effects on growth and body weight while DBEM-Maxent and DBEM-Aquamaps do not consider them, explaining some of the differences in the projections between the models. Regional differences in variability in projected potential catches between different DBEM configurations can be directly attributed to differences in the implementation of the species distribution models and hence to their sensitivity to changes in ocean conditions. This is particularly the case in tropical regions where ocean conditions are generally at the edges of species' environmental preferences, and where environmental conditions (e.g., sea surface temperature) start to exceed the historical ranges early in the 21st century (Rodgers et al., 2015).

The long-term changes in projected catches were particularly large relative to the variability between models in tropical and high latitude regions. Previous studies applied DBEM-Basic to project changes in catches in the Arctic (Lam et al., 2014), UK (Jones et al., 2015), the Northeast Pacific (Cheung et al., 2015) and the Northeast Atlantic (Cheung et al., 2011). Our results suggest that the qualitative patterns of changes in catch potential across these broad ocean regions may not be affected by the structural uncertainty of DBEM explored herein. The standard deviation of the projected changes in catch potential across DBEM versions in these regions were small relative to the mean changes in these regions. However, there is a need to further quantify the uncertainties associated with these projections as the magnitude of changes in potential catch varied between models. Further exploration of DBEM algorithm uncertainty with developing higher-resolution ESMs may also reveal departures at finer scales that were not resolved herein.

This study provided evidence to indicate that the macroecological relationship between ocean productivity, available habitat, and catch was generally robust to alternative fish models (Plagányi, 2007): each alternative DBEM implementation produced robust correlations with observed maximum catch across LMEs. All algorithm variants, however, were also notable for their deficiencies in capturing catches in the most productive regions and for large discrepancies in Arctic and Antarctic waters. There are likely several factors contributing to these discrepancies. First, ESM2M does reasonably well in capturing cross-LME variations in NPP ($r=0.73$), but the coarse resolution does not allow full representation of energetic coastal processes that contribute to the productivity of these systems. Eastern boundary upwelling, for example, is poorly captured (e.g., Stock et al., 2011). Second, the connection between primary production and fisheries across vastly different ecosystems is complicated by planktonic food web dynamics (Ryther, 1969). Recent work has suggested mesozooplankton or export production as potentially more robust metrics of fisheries capacity than NPP (Friedland et al., 2012). Both of these quantities exhibit sharper gradients between ecosystems than NPP (Stock et al., 2014b) that may improve slopes in Fig. 2. They also feature sharper projected trends under climate change (Bopp et al., 2013; Stock et al., 2014a).

Exploring the implications of such improvements is left to future work.

In the Arctic, fisheries were under-developed and substantially under-reported (Zeller et al., 2011). Arctic systems are thus often omitted from studies relating potential catch and ocean productivity (Chassot et al., 2010; Friedland et al., 2012), explaining why predicted catches from DBEM were higher than reported catches in the Arctic.

Given the variation in the projections between different DBEM versions, this study shows that multiple version of DBEM should be used to quantify the structural uncertainty of the models and to capture all the potential range of responses of the species to environmental changes. Particularly, in regions where the models diverge substantially in their projections, there is a need to better understand the key processes and variables during the changes in fish stocks, and select the appropriate model structure that best represents these processes. Weighting of the model outputs may be considered, for example, based on the quality of the prediction of present species distribution with regards to data using Area Under the Curve (AUC) index or true skill score (TSS) (Meller et al., 2014). However, this requires more substantial testing of the skills of the models before appropriate weighting to each model could be made. Without further information about the relative performance of each DBEM model, their outputs could be weighted equally.

Overall, findings from this analysis should contribute to the quantification of the cascade of uncertainty associated with living marine resources projections that includes internal variability, model uncertainties and scenario uncertainties (Cheung et al., 2016). Specifically, this study focused on the structural uncertainty of DBEM—one of the few approaches that had generated global projections of fisheries catches under climate change. Other aspects of projection uncertainties were not explored here, including uncertainties associated with projected changes in ocean properties, the effects of other biological mechanisms such as evolutionary and transgenerational adaptations and trophic interactions, and variations in fishing scenarios. Future studies should incrementally address these different aspects of uncertainty. Ultimately, this would improve our understanding about the possible future changes in marine fish stocks under climate change and facilitate further exploration of policies to mitigate and adapt to these changes.

Acknowledgements

This study is a contribution from the Nippon Foundation—The University of British Columbia Nereus Program. WWLC also acknowledges funding support from Natural Sciences and Engineering Research Council of Canada (22R68146). T. L. Frölicher acknowledges financial support from the SNSF (Ambizione grant PZ00P2_142573).

Appendix A. Supplementary data

Supplementary data associated with this article can be found, in the online version, at <http://dx.doi.org/10.1016/j.ecolmodel.2015.12.018>.

References

- Ainsworth, C.H., Samhouri, J.F., Busch, D.S., Cheung, W.W.L., Dunne, J., Okey, T.A., 2011. Potential impacts of climate change on Northeast Pacific marine foodwebs and fisheries. *ICES J. Mar. Sci.* 68, 1217–1229.
- Barange, M., Merino, G., Blanchard, J.L., Scholtens, J., Harle, J., Allison, E.H., Allen, J.I., Holt, J., Jennings, S., 2014. Impacts of climate change on marine ecosystem production in societies dependent on fisheries. *Nat. Clim. Change* 4, 211–216.

- Beaugrand, G., Edwards, M., Raybaud, V., Goberville, E., Kirby, R.R., 2015. Future vulnerability of marine biodiversity compared with contemporary and past changes. *Nat. Clim. Change* 5, 695–701.
- Bopp, L., Resplandy, L., Orr, J.C., Doney, S.C., Dunne, J.P., Gehlen, M., Halloran, P., Heinze, C., Ilyina, T., Séférian, R., Tjiputra, J., Vichi, M., 2013. Multiple stressors of ocean ecosystems in the 21st century: projections with CMIP5 models. *Biogeosciences* 10, 6225–6245.
- Chassot, E., Bonhommeau, S., Dulvy, N.K., Mélin, F., Watson, R., Gascuel, D., Le Pape, O., 2010. Global marine primary production constrains fisheries catches. *Ecol. Lett.* 13, 495–505.
- Chen, Y., Hunter, M., Vadas, R., Beal, B., 2003. Developing a growth-transition matrix for the stock assessment of the green sea urchin (*Strongylocentrotus droebachiensis*) off Maine. *Fish. Bull.* 101, 737–744.
- Cheung, W.W., Brodeur, R.D., Okey, T.A., Pauly, D., 2015. Projecting future changes in distributions of pelagic fish species of Northeast Pacific shelf seas. *Prog. Oceanogr.* 130, 19–31.
- Cheung, W.W., Watson, R., Pauly, D., 2013a. Signature of ocean warming in global fisheries catch. *Nature* 497, 365–368.
- Cheung, W.W.L., Sumaila, U.R., 2015. Economic incentives and overfishing: a bioeconomic vulnerability index. *Mar. Ecol. Prog. Ser.* 530, 223–232.
- Cheung, W.W.L., Sarmiento, J.L., Dunne, J., Frölicher, T.L., Lam, V.W.Y., Deng Palomares, M.L., Watson, R., Pauly, D., 2013b. Shrinking of fishes exacerbates impacts of global ocean changes on marine ecosystems. *Nat. Clim. Change* 3, 254–258.
- Cheung, W.W.L., Close, C., Lam, V., Watson, R., Pauly, D., 2008a. Application of macroecological theory to predict effects of climate change on global fisheries potential. *Mar. Ecol. Prog. Ser.* 365, 187–197.
- Cheung, W.W.L., Lam, V., Pauly, D. (Eds.), 2008b. Modelling Present and Climate-shifted Distributions of Marine Fishes and Invertebrates. Fisheries Centre Research Reports, vol. 16(3), pp. 1–72.
- Cheung, W.W.L., Lam, V.W.Y., Pauly, D., 2008c. Dynamic bioclimate envelope model to predict climate-induced changes in distribution of marine fishes and invertebrates. In: Cheung, W.W.L., Lam, V.W.Y., Pauly, D. (Eds.), Modelling Present and Climate-shifted Distributions of Marine Fishes and Invertebrates, vol. 16(3). University of British Columbia, Vancouver, pp. 5–50.
- Cheung, W.W.L., Dunne, J., Sarmiento, J.L., Pauly, D., 2011. Integrating ecophysiology and plankton dynamics into projected maximum fisheries catch potential under climate change in the Northeast Atlantic. *ICES J. Mar. Sci.* 68, 1008–1018.
- Cheung, W.W.L., Frölicher, T.L., Asch, R.G., Jones, M.C., Pinsky, M.L., Reygondeau, G., Rodgers, K.B., Rykaczewski, R.R., Sarmiento, J.L., Stock, C., Watson, J.R., 2016. Building confidence in projections of the responses of living marine resources to climate change. *ICES J. Mar. Sci.*, <http://dx.doi.org/10.1093/icesjms/fsv250>.
- Cheung, W.W.L., Lam, V.W.Y., Sarmiento, J.L., Kearney, K., Watson, R., Pauly, D., 2009. Projecting global marine biodiversity impacts under climate change scenarios. *Fish Fish.* 10, 235–251.
- Cheung, W.W.L., Lam, V.W.Y., Sarmiento, J.L., Kearney, K., Watson, R.E.G., Zeller, D., Pauly, D., 2010. Large-scale redistribution of maximum fisheries catch potential in the global ocean under climate change. *Global Change Biol.* 16, 24–35.
- Close, C., Cheung, W.W.L., Hodgson, S., Lam, V., Watson, D., Pauly, D., 2006. Distribution ranges of commercial fishes and invertebrates. In: Palomares, D., Stergiou, K.I., Pauly, D. (Eds.), Fishes in Databases and Ecosystems, vol. 14(4). University of British Columbia, Vancouver, pp. 27–37.
- Dunne, J.P., John, J.G., Sheviakova, E., Stouffer, R.J., Krasting, J.P., Malyshev, S.L., Milly, P.C.D., Sentman, L.T., Adcroft, A.J., Cooke, W., Dunne, K.A., Griffies, S.M., Hallberg, R.W., Harrison, M.J., Levy, H., Wittenberg, A.T., Phillips, P.J., Zadeh, N., 2012. GFDL's ESM2 global coupled climate–carbon earth system models. Part II: carbon system formulation and baseline simulation characteristics. *J. Climate* 26, 2247–2267.
- Elith, J., Leathwick, J.R., 2009. Species distribution models: ecological explanation and prediction across space and time. *Annu. Rev. Ecol. Evol. Syst.* 40, 677.
- Elith, J., Phillips, S.J., Hastie, T., Dudík, M., Chee, Y.E., Yates, C.J., 2011. A statistical explanation of MaxEnt for ecologists. *Divers. Distrib.* 17, 43–57.
- Escoufier, Y., 1970. Echantillonage dans une population de variables aléatoires réelles. *Department de math.; Univ. des sciences et techniques du Languedoc*.
- Fernandes, J.A., Cheung, W.W., Jennings, S., Butenschön, M., Mora, L., Frölicher, T.L., Barange, M., Grant, A., 2013. Modelling the effects of climate change on the distribution and production of marine fishes: accounting for trophic interactions in a dynamic bioclimate envelope model. *Global Change Biol.* 19, 2596–2607.
- Friedland, K.D., Stock, C., Drinkwater, K.F., Link, J.S., Leaf, R.T., Shank, B.V., Rose, J.M., Pilskaln, C.H., Fogarty, M.J., 2012. Pathways between primary production and fisheries yields of large marine ecosystems. *PLoS ONE* 7, e28945.
- Froese, R., Pauly, D., 2011. FishBase, (www.fishbase.org) (accessed Feb. 2011).
- Gattuso, J.-P., Magnan, A., Billé, R., Cheung, W., Howes, E., Joos, F., Allemand, D., Bopp, L., Cooley, S., Eakin, C.M., Hoegh-Guldberg, O., Kelly, R.P., Pörtner, H.-O., Rogers, A.D., Baxter, J.M., Laffoley, D., Osborn, D., Rankovic, A., Rochette, J., Sumaila, U.R., Treyer, S., Turley, C., 2015. Contrasting futures for ocean and society from different anthropogenic CO₂ emissions scenarios. *Science* 349, aac4722.
- Haddon, M., 2010. Modelling and Quantitative Methods in Fisheries. CRC Press, Boca Raton, London, New York.
- IPCC, 2013. Summary for policy makers. In: Stocker, T.F., Qin, D., Plattner, G.-K., Tignor, M., Allen, S.K., Boschung, J., Nauels, A., Xia, Y., Bex, V., Midgley, P.M. (Eds.), Cambridge University Press, Cambridge, United Kingdom and New York, NY, USA.
- Jones, M., Dye, S., Pinngar, J., Warren, R., Cheung, W.W.L., 2012. Modelling commercial fish distributions: prediction and assessment using different approaches. *Ecol. Modell.* 225, 133–145.
- Jones, M.C., Cheung, W.W.L., 2015. Multi-model ensemble projections of climate change effects on global marine biodiversity. *ICES J. Mar. Sci.* 72, 741–752.
- Jones, M.C., Dye, S.R., Pinngar, J.K., Warren, R., Cheung, W.W.L., 2015. Using scenarios to project the changing profitability of fisheries under climate change. *Fish Fish.* 16, 603–622.
- Kaschner, K., Tittensor, D.P., Ready, J., Gerrodette, T., Worm, B., 2011. Current and future patterns of global marine mammal biodiversity. *PLoS ONE* 6, e19653.
- Kirby, R.R., Beaugrand, G., 2009. Trophic amplification of climate warming. *Proc. R. Soc. London, Ser. B: Biol. Sci.* 276, 4095–4103, rspb20091320.
- Lam, V.W.Y., Cheung, W.W.L., Sumaila, U.R., 2014. Marine capture fisheries in the Arctic: winners or losers under climate change and ocean acidification? *Fish Fish.*, <http://dx.doi.org/10.1111/faf.12106>.
- Meller, L., Cabeza, M., Pironon, S., Barbet-Massin, M., Maiorano, L., Georges, D., Thuiller, W., 2014. Ensemble distribution models in conservation prioritization: from consensus predictions to consensus reserve networks. *Divers. Distrib.* 20, 309–321.
- Nahas, E.L., Jackson, G., Pattiarratchi, C.B., Ivey, G.N., 2003. Hydrodynamic modelling of snapper *Pagrus auratus* egg and larval dispersal in Shark Bay, Western Australia: reproductive isolation at a fine spatial scale. *Mar. Ecol. Prog. Ser.* 265, 213–226.
- O'Connor, M.I., Bruno, J.F., Gaines, S.D., Halpern, B.S., Lester, S.E., Kinlan, B.P., Weiss, J.M., 2007. Temperature control of larval dispersal and the implications for marine ecology, evolution, and conservation. *Proc. Natl. Acad. Sci. U.S.A.* 104, 1266–1271.
- Pauly, D., 1980. On the interrelationships between natural mortality, growth parameters and mean environmental temperature in 175 fish stocks. *J. Cons., Cons. Int. Explor. Mer* 39, 175–192.
- Pauly, D., 1981. The relationship between gill surface area and growth performance in fish: a generalization of von Bertalanffy's theory of growth. *Ber. Dtsch. Wiss. Komm. Meeresforsch.* 28, 251–282.
- Pauly, D., 2010. Gasping Fish and Panting Squids: Oxygen, Temperature and the Growth of Water-Breathing Animals. International Ecology Institute, Oldendorf/Luhe.
- Phillips, S.J., Anderson, R.P., Schapire, R.E., 2006. Maximum entropy modeling of species geographic distributions. *Ecol. Modell.* 190, 231–259.
- Phillips, S.J., Dudík, M., 2008. Modeling of species distributions with Maxent: new extensions and a comprehensive evaluation. *Ecography* 31, 161–175.
- Pinsky, M.L., Worm, B., Fogarty, M.J., Sarmiento, J.L., Levin, S.A., 2013. Marine taxa track local climate velocities. *Science* 341, 1239–1242.
- Plagányi, É.E., 2007. Models for an Ecosystem Approach to Fisheries. Food & Agriculture Org.
- Poloczanska, E.S., Brown, C.J., Sydeman, W.J., Kiessling, W., Schoeman, D.S., Moore, P.J., Brander, K., Bruno, J.F., Buckley, L.B., Burrows, M.T., Duarte, C.M., Halpern, B.S., Holding, J., Kappel, C.V., O'Connor, M.I., Pandolfi, J.M., Parmesan, C., Schwinger, F., Thompson, S.A., Richardson, A.J., 2013. Global imprint of climate change on marine life. *Nat. Clim. Change* 3, 919–925.
- Portner, H.-O., Karl, D.M., Boyd, P.W., Cheung, W.W.L., Lluch-Cota, S.E., Nojiri, Y., Schmidt, D.N., Zavialov, P.O., Alheit, J., Aristegui, J., 2014. Chapter 6: Ocean systems. In: Field, C.B., Barros, V.R., Dokken, D.J., Mach, K.J., Mastrandrea, M.D., Bilir, T.E., Chatterjee, M., Ebi, K.L., Estrada, Y.O., Genova, R.C., Girma, B., Kissel, E.S., Levy, A.N., MacCracken, S., Mastrandrea, P.R., White, L.L. (Eds.), Climate Change 2014: Impacts, Adaptation, and Vulnerability. Part A: Global and Sectoral Aspects. Contribution of Working Group II to the Fifth Assessment Report of the Intergovernmental Panel on Climate Change. Cambridge University Press, Cambridge.
- Ready, J., Kaschner, K., South, A.B., Eastwood, P.D., Rees, T., Rius, J., Agbayani, E., Kullander, S., Froese, R., 2010. Predicting the distributions of marine organisms at the global scale. *Ecol. Modell.* 221, 467–478.
- Rengstorf, A.M., Yesson, C., Brown, C., Grehan, A.J., 2013. High-resolution habitat suitability modelling can improve conservation of vulnerable marine ecosystems in the deep sea. *J. Biogeogr.* 40, 1702–1714.
- Rodgers, K.B., Lin, J., Frölicher, T.L., 2015. Emergence of multiple ocean ecosystem drivers in a large ensemble suite with an earth system model. *Biogeosciences* 11, 18189–18227.
- Ryther, J.H., 1969. Photosynthesis and fish production in the sea. *Science* 166, 72–76.
- Sadovy, Y., Punt, A.E., Cheung, W.L., Vasconcellos, M., Suharti, S., Mapstone, B.D., 2007. Stock assessment approach for the Napoleon fish, *Cheilinus undulatus*, in Indonesia. A tool for quota setting for data-poor fisheries under CITES Appendix II Non-Detriment Finding requirements. In: FAO Fisheries Circular No. 1023. FAO, Rome, pp. 71.
- Shannon, C.E., 2001. A mathematical theory of communication. *ACM SIGMOBILE Mob. Comput. Commun. Rev.* 5, 3–55.
- Stock, C.A., Alexander, M.A., Bond, N.A., Brander, K.M., Cheung, W.W.L., Curchitser, E.N., Delworth, T.L., Dunne, J.P., Griffies, S.M., Haltuch, M.A., Hare, J.A., Hollowed, A.B., Lehodey, P., Levin, S.A., Link, J.S., Rose, K.A., Rykaczewski, R.R., Sarmiento, J.L., Stouffer, R.J., Schwinger, F.B., Vecchi, G.A., Werner, F.E., 2011. On the use of IPCC-class models to assess the impact of climate on Living Marine Resources. *Prog. Oceanogr.* 88, 1–27.
- Stock, C., Dunne, J., John, J., 2014a. Drivers of trophic amplification of ocean productivity trends in a changing climate. *Biogeosciences* 11, 7125–7135.
- Stock, C.A., Dunne, J.P., John, J.G., 2014b. Global-scale carbon and energy flows through the marine planktonic food web: an analysis with a coupled physical–biological model. *Prog. Oceanogr.* 120, 1–28.
- Zeller, D., Booth, S., Pakhomov, E., Swartz, W., Pauly, D., 2011. Arctic fisheries catches in Russia, USA, and Canada: baselines for neglected ecosystems. *Polar Biol.* 34, 955–973.